

## Supramolecular structural control: photochemical reactions between styrylpyridine derivative and cucurbit[7,8]urils

Received 00th January 20xx,  
Accepted 00th January 20xx

Shang-Wei Yuan,<sup>[a]</sup> Heng Wu,<sup>[a]</sup> Xi Nan Yang,<sup>[a]</sup> Mao-Xia Yang,<sup>[a]</sup> Yang Luo,<sup>[a]</sup> Wen Min,<sup>[a]</sup> Zhen-Feng Lu,<sup>[a]</sup> Carl Redshaw,<sup>[b]</sup> Zhu Tao<sup>[a]</sup>, Xin Xiao<sup>\*[a]</sup>

DOI: 10.1039/x0xx00000x

The use of cucurbit[*n*]urils to control the photochemical reactions of styrylpyridine salts has become a new strategy in supramolecular chemistry. In an aqueous solution, styrylpyridine derivatives (CHP) can form supramolecular complexes of the 1:2 and 2:1 type with cucurbit[8]uril (Q[8]) and cucurbit[7]uril (Q[7]), respectively. Given the photosensitivity of the CHP, the C=C bond of the CHP undergoes a *cis-trans* isomerization reaction and a [2+2] cycloaddition reaction under 365 nm UV irradiation in aqueous solution. After binding with Q[8], the photo-induced [2+2] cycloaddition reaction rate of the CHP is greatly increased, while after binding with Q[7], the C=C bond of the CHP only undergoes a *cis-trans* isomerization reaction, *i.e.* no further photo-induced [2+2] cycloaddition reaction occurs. Competitive experiments demonstrated that CHP is more inclined to combine with Q[7], and thus when Q[7] and Q[8] coexist in the system, the inhibition of the [2+2] cycloaddition reaction of CHP by Q[7] is not disrupted. The characteristics of this supramolecular catalysis and supramolecular protection make it applicable to catalyze or inhibit reactions required under specific circumstances.

### 1. Introduction

The construction of stimuli-response molecular devices and molecular machines is a huge challenge<sup>[1]</sup>, and there are many kinds of molecular machines in nature<sup>[2,3]</sup>. One of the main tasks of biomolecular machines is to synthesize other molecules, which can be achieved by precise control of chemical reactions through complex catalysis<sup>[4-6]</sup>. An in-depth understanding of biomolecular machines has encouraged scientists to develop and synthesize various artificial molecular machines to perform predictable tasks via mechanical motion at the molecular level<sup>[7]</sup>. For example, it is possible to create complex functional substances by controlling the structure and dynamic characteristics of self-assembly<sup>[8-9]</sup>. Molecular machines are intrinsically not only very suitable for performing these control tasks, but can also perform other multifaceted functions, such as act as smart molecular receptors and sensors<sup>[10-11]</sup>, supramolecular drug delivery systems<sup>[12-13]</sup>, controllable catalysts<sup>[14]</sup>, and other complex stimuli-response materials<sup>[15,16]</sup>. Thus, the use of external stimuli to control the binding dynamics in supramolecular systems is critical to the development of advanced molecular machines and equipment. Macrocyclic host molecules are one of the most popular building blocks for constructing supramolecular systems because of their ability to recognize various complementary guest molecules or ions<sup>[17]</sup>. The cucurbit[*n*]urils (Q[*n*]s) are a

symmetric macrocyclic family of molecules containing a hydrophobic cavity and two carbonyl portals, which exhibit significant affinity for suitable guests or ions in aqueous solution<sup>[18-28]</sup>. The external control of supramolecular systems has attracted wide interest in many scientific disciplines<sup>[29-31]</sup>. The reversible control of the host-guest complex state by using light has become an important focus, as it is not limited by time and space and allows for remote manipulation triggered without any chemical waste<sup>[32]</sup>. Photosensitive organic molecules, such as azobenzene, styrylpyridine, dithiophene ethylene, anthracene, spiropyran, and their derivatives, have been central to the development of a series of photosensitive materials and self-assembly systems. Therefore, such a photosensitive compound can be included as a guest in a macrocyclic host molecule (such as Q[*n*]) to obtain a photosensitive host-guest complex<sup>[33,34]</sup>. Q[8] can combine with two identical or different aromatic molecules of specific structure at the same time to form a ternary host-guest complex due to its large cavity, which makes the reaction substrates for the Q[8] system particularly abundant. Sivaguru *et al.* have used Q[8] to regulate the photocycloaddition reaction of coumarin compounds<sup>[35]</sup>. On the other hand, molecular cages and macrocyclic molecules can act both as supramolecular catalysts to promote certain specific reactions and as supramolecular inhibitors to inhibit certain reactions of the guest molecule by binding to it or as supramolecular protectors of the assembly behavior<sup>[36,37]</sup>. For example, Zhang's group<sup>[38]</sup> proposed a strategy to control the reactivity of the Se-Se bond by using cucurbit[*n*]uril supramolecular chemistry. The Hu<sup>[39]</sup> group reported the host-guest complexation of anthracene derivatives with Q[*n*]s, and the photoreactions of these derivatives in the presence of Q[*n*]s. Both Q[8] and Q[10] acted as supramolecular nanoreactors and

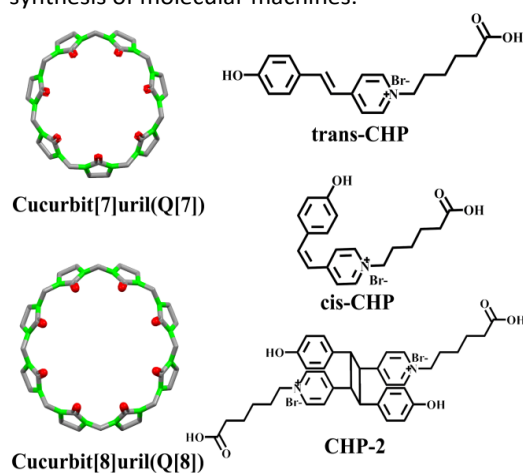
<sup>a</sup> Key Laboratory of Macrocyclic and Supramolecular Chemistry of Guizhou Province, Institute of Applied Chemistry, Guizhou University, Guiyang 550025, China

<sup>b</sup> Department of Chemistry, University of Hull, Hull HU6 7RX, U.K

<sup>\*[a]</sup> Corresponding author Email: gyhxixiao@163.com

catalysts in the photoreaction of anthracene derivatives. However, Q[10] promoted the photodimerization of guests. Tang<sup>[40]</sup> and co-workers studied the behavior of the *trans*-1-methyl-4-(4-hydroxystyryl)pyridinium cation (HSP<sup>+</sup>) to Q[6] in the presence of Na<sup>+</sup> cations, which created a conceptual framework for using such nonlinearities to control multistep reactions in cucurbit[*n*]uril chemistry.

Herein, the styrylpyridine derivative CHP was synthesized by accessing 6-bromohexanoic acid with (*E*)-4-(2-(pyridin-4-yl)vinyl)phenol. Styrylpyridine is a well-known photochromic compound<sup>[40]</sup>, which can be efficiently isomerized by UV light from the thermodynamically stable *E* form to the *Z* isomer and can also undergo [2+2] cycloaddition reactions. In the present work, supramolecular assemblies between Q[7], Q[8], and CHP are investigated by NMR spectroscopy, fluorescence spectroscopy, UV-Vis spectroscopy, and isothermal titration calorimetry, and their photostimulation responsiveness is further studied. The results show that in an aqueous solution, Q[8] accelerates the [2+2] cycloaddition reaction of CHP, while the inclusion of Q[7] inhibits the [2+2] cycloaddition reaction of CHP without affecting its *cis-trans* isomerization reaction. Such a process has potential applications for the development and synthesis of molecular machines.



Scheme 1. Structural representations of Q[7], Q[8], *trans*-CHP, *cis*-CHP, and CHP-2.

## 2. Results and discussion

### 2.1 Host-guest interaction of CHP with Q[7] and Q[8]

Styrylpyridine salts can mostly undergo two main types of photochemical reactions: photocatalytic *cis-trans* isomerization and photocatalytic [2+2] cycloaddition reactions. In general, *cis-trans* isomerization reactions are mainly unimolecular reactions, involving the rotation of intramolecular covalent bonds, affected by the viscosity of the solution, but not very sensitive to the concentration of the reactants. By contrast, photo-induced [2+2] cycloaddition reactions are bimolecular reactions, more sensitive to the concentration of the reactants, and more likely to occur at higher concentrations. To study the effect of Q[*n*]s on the photochemical reaction of CHP molecules, the host-guest interaction of Q[7] and Q[8] with CHP was first studied.

#### 2.1.1 Analysis of the interaction between CHP and Q[8]

Characterization methods such as <sup>1</sup>H NMR spectroscopy, UV-vis spectroscopy, and fluorescence emission spectroscopy were used to verify the existence of the interaction between CHP and Q[8]. The interaction between the guest CHP and Q[8] was studied by <sup>1</sup>H NMR spectroscopy data recorded in D<sub>2</sub>O solution. Figure 1a shows the changes in the <sup>1</sup>H NMR spectra of CHP protons with the addition of certain amounts of Q[8] to the solution. When 0.5 equivalent of Q[8] is added, the signals of the protons H<sub>a</sub>, H<sub>b</sub>, H<sub>c</sub>, H<sub>d</sub>, H<sub>e</sub>, H<sub>f</sub>, and H<sub>g</sub> of CHP were observed to shift upfield, while the signals of the protons H<sub>h</sub>, H<sub>i</sub>, H<sub>j</sub> and H<sub>k</sub> of the alkyl chain shift downfield slightly, indicating that the CHP-phenyl and the quaternary ammonium are included in the cavity of Q[8], and the alkyl chain is located at the portal of Q[8] (see the cartoon in the upper right corner of the figure), forming a 1:2 host-guest inclusion complex.

Figure 1. (a) <sup>1</sup>H NMR spectra (400 MHz, D<sub>2</sub>O) of free CHP (5 × 10<sup>-4</sup> mol · L<sup>-1</sup>) (I), Q[8]-CHP (II) and free Q[8] (III); (b) UV absorption spectra of CHP (2.0 × 10<sup>-5</sup> mol · L<sup>-1</sup>), with the increase of Q[8] (0, 0.1, 0.2, ..., 0.8, 0.9, 1.0 equivalents); (c) Fluorescence spectra of CHP (2.0 × 10<sup>-5</sup> mol · L<sup>-1</sup>), with the increase of Q[8] (0, 0.1, 0.2 ... to 0.8, 0.9, 1.0 equivalents)

To further understand the binding of guest CHP with Q[8], UV-vis spectra were obtained by using an aqueous solution containing a fixed concentration of guest CHP and a variable concentration of Q[8] with the maximum absorption of guest CHP concentrated at 344 nm (Figure 1b and S5). With the gradual increase of Q[8] concentration, due to the formation of the host-guest complex, the system's UV absorption intensity gradually decreases, which tends to be flat when the ratio of the amount of host and guest substances is close to 1:2 (N<sub>Q[8]</sub>/N<sub>CHP</sub>), indicating that the host and guest formed an inclusion complex with an actual ratio of 1:2, which was further confirmed by the Jobs method. In addition, a similar experiment was performed on the fluorescence emission spectroscopy as shown in Figures 1c and S6, where the fluorescence emission of CHP in an aqueous solution occurs at 457 nm with an excitation wavelength of 350 nm. When Q[8] is gradually added to the solution of guest CHP, the intensity of the emission spectra of CHP will gradually increase with the increase of the N<sub>Q[8]</sub>/N<sub>CHP</sub> ratio, accompanied by a significant red shift. The fluorescence data can be fitted to a 1:2 binding model and at the same time, the Job's plot further proves the host-guest interaction ratio of 1:2. From the ITC data, the overall binding constant (K<sub>a</sub>) for the complexation of the CHP guest with the Q[8] host was calculated at 1.832 × 10<sup>12</sup> M<sup>-2</sup>, with K<sub>a1</sub> at 3.951 × 10<sup>6</sup> M<sup>-1</sup> (Figure S7).

### 2.1.2 Analysis of the interaction between CHP and Q[7]

Compare with the Q[8] system, the host-guest complex between Q[7] with CHP is different. As shown in the  $^1\text{H}$  NMR spectrum (Figure 2a), when Q[7] is added to CHP, the protons  $\text{H}_c$ ,  $\text{H}_d$ ,  $\text{H}_e$ ,  $\text{H}_f$ ,  $\text{H}_g$ ,  $\text{H}_h$ ,  $\text{H}_i$ ,  $\text{H}_j$ , and  $\text{H}_k$  of the guest CHP shift upfield by 0.06, 0.04, 0.14, 0.44, 0.52, 0.67, 0.57, 0.45, and 0.30 ppm, respectively, indicating that the C=C bonds, quaternary ammonium and alkyl chains of CHP enter into the Q[7] cavity, which is shielded by Q[7]. In addition,  $\text{H}_a$  and  $\text{H}_b$  shift downfield by 0.02 and 0.04 ppm, respectively, indicating that the benzene ring and hydroxyl of the guest are located outside the portal of Q[7].

**Figure 2.** (a)  $^1\text{H}$  NMR spectra (400 MHz,  $\text{D}_2\text{O}$ ) of free CHP ( $5 \times 10^{-4} \text{ mol} \cdot \text{L}^{-1}$ ) (I), Q[7]-CHP (II) and free Q[7] (III,  $5.0 \times 10^{-4} \text{ mol} \cdot \text{L}^{-1}$ ); (b) UV absorption spectra of CHP ( $2.0 \times 10^{-5} \text{ mol} \cdot \text{L}^{-1}$ ), with the increase of Q[7] (0, 0.2, 0.4, ..., 3.6, 3.8, 4.0 equivalents); (c) Fluorescence spectra of CHP ( $2.0 \times 10^{-5} \text{ mol} \cdot \text{L}^{-1}$ ), with the increase of Q[7] (0, 0.2, 0.4, ..., 3.6, 3.8, 4.0 equivalents).

To further confirm the binding ratio of the interaction between CHP and Q[7], the changes of the UV absorption spectra of Q[7]-CHP with the concentration of host and guest and the trend with the ratio of host and guest at a wavelength of 344 nm were investigated, as shown in Figures 2b and S9. On fixing the concentration of the guest, with the gradual increase of the concentration of Q[7], the UV absorption intensity of the Q[7]-CHP system gradually decreases, which tends to be flat when the ratio of the amount of host and guest substances is close to 2:1, indicating that the host and guest form an inclusion complex with a host-guest ratio of 2:1, which further confirmed by the Jobs method. In addition, the fluorescence spectroscopy further demonstrates that Q[7] and CHP form a 2:1 host-guest inclusion complex (Figures 2c and S12). It is worth mentioning that according to an analysis of the NMR spectroscopic results, the shuttle of a Q[7] molecule on the CHP molecule also needs to be considered. From the ITC data,  $K_a$  of the CHP guest with the Q[7] host was calculated at  $1.553 \times 10^{13} \text{ M}^{-2}$ , with  $K_{a1}$  at  $5.249 \times 10^7 \text{ M}^{-1}$  (Figure S13), which is significantly greater than the  $K_a$  calculated for Q[8].

### 2.2 Effect of Q[n] on the photochemical reaction of CHP

The foregoing experiments verify that CHP forms a host-guest complex with Q[8] and Q[7] in a molar ratio of 1:2, 2:1 ( $N_{\text{Q}[n]}/N_{\text{CHP}}$ ), respectively, and then by applying 365 nm ultraviolet radiation to the system (the wavelength of all ultraviolet radiation mentioned in this

article is 365 nm) to study the influence of Q[8] and Q[7] on the photoreaction of CHP was studied.

$^1\text{H}$  NMR spectroscopy was first employed to characterize the photochemical behavior of the guest molecule CHP. As shown in Figure 3a, without illumination by ultraviolet light, there are 6 groups of signals in the aromatic region of the spectrum, which belong to 4 types of hydrogen nuclei of the aromatic ring and 2 double bond hydrogen nuclei. In the beginning, all the guest molecules of CHP in the system are in a *trans* configuration (*trans*-CHP). *Trans*-CHP was irradiated with 365 nm wavelength ultraviolet radiation and the changes in the proton NMR spectra were recorded. The *cis*-CHP signal is observed in the spectra after the 30s of irradiation, and the signal intensity of the *trans*-configuration is significantly reduced. When the irradiation is continued for 10 minutes, the initial *trans*-CHP is almost converted completely to *cis*-CHP. On this basis, the sample was continuously irradiated with UV irradiation, and the formation of the characteristic peak of a dimer (CHP-2) is observed at 60 min, and when the irradiation duration is extended to 180min, CHP is almost completely converted to a dimer and the *cis*-CHP signal is only faintly visible.

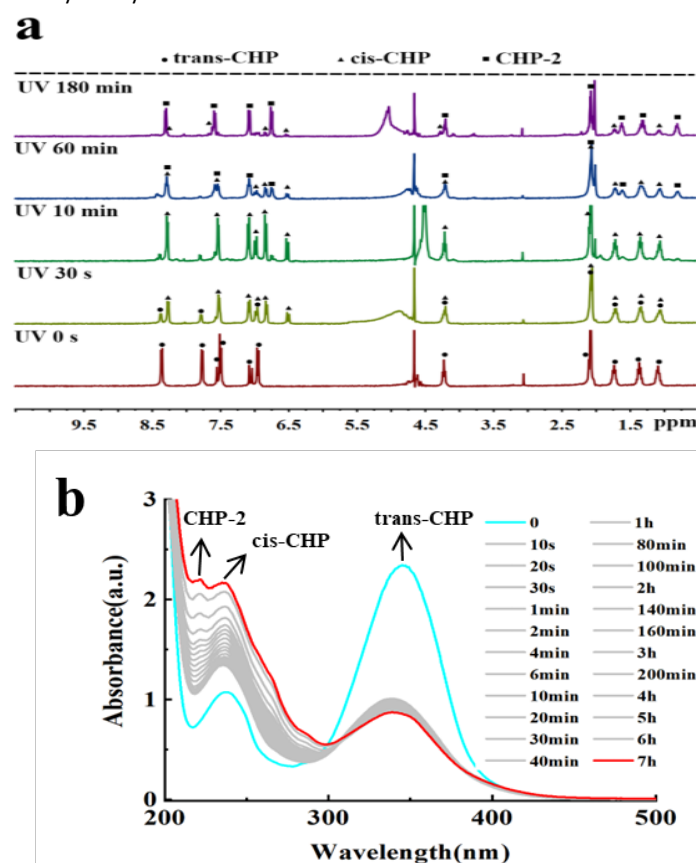


**Figure 3.** (a)  $^1\text{H}$  NMR spectra of CHP ( $5 \times 10^{-4} \text{ mol} \cdot \text{L}^{-1}$ ) with different irradiation durations; (b) UV-Vis spectra of CHP ( $1 \times 10^{-4} \text{ mol} \cdot \text{L}^{-1}$ ) solution with UV irradiation.

UV-vis absorption spectroscopy was also used to characterize the photochemical behavior of the molecular CHP itself. As shown in Figure 3b, the maximum absorption intensity of CHP solution at 345 nm under 365 nm ultraviolet light irradiation decreases on prolonged irradiation, and the absorbance near 237 nm gradually increases. The intensity change of each absorption peak reflects the transformation of the intramolecular conjugate structure (from the *trans* to *cis* configuration) in the system under ultraviolet light irradiation. With the continuous irradiation of ultraviolet light, a new absorption peak

appears near 222 nm, attributed to the dimer product CHP-2 formed by the photodimerization of CHP. However, it is worth noting that after several hours of irradiation, the absorption peak at 345 nm still maintains an absorbance of about 0.86, indicating that the CHP reactant is still present.

### 2.2.1 Photodimerization of CHP catalyzed by Q[8]

To better improve the conversion efficiency of the dimer product CHP-2 from photodimerization, 5% Q[8] solution was added and the UV irradiation and NMR detection was conducted under the same conditions. Consistent with the pure CHP solution, CHP undergoes a process of transformation from *trans*-CHP to *cis*-CHP, and finally converting to dimer (CHP-2). However, in the presence of Q[8], the entire process can be completed within 10 min. As shown in Figure 4, in the NMR spectra of the sample irradiated for 10 seconds, the signals of *trans*-CHP, *cis*-CHP, and dimer (CHP-2) can be observed at the same time. After the irradiation duration is extended to 10 min, the spectrum is dominated by the signals of the hydrogen nuclei of the four groups of aromatic rings belonging to the dimer CHP-2; the signals for *trans*-CHP and *cis*-CHP are faintly visible, and their intensity is greatly weakened and almost submerged in the background noise. It can be seen that the role of Q[8] in this system is that of a catalyst.

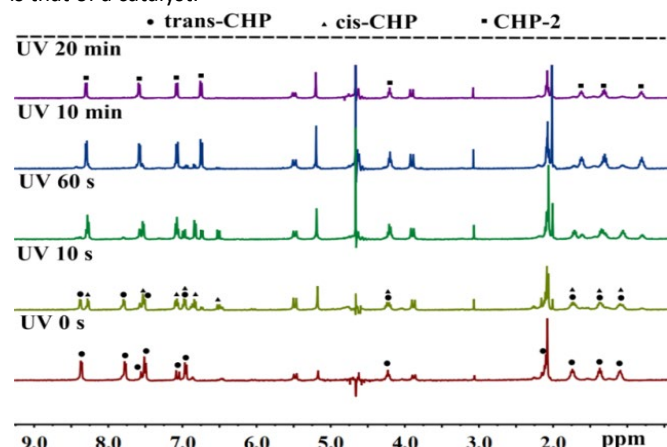


Figure 4.  $^1\text{H}$  NMR spectra of CHP solutions ( $5 \times 10^{-4} \text{ mol L}^{-1}$ ) containing 5% Q[8] with different irradiation durations.

Table 1. The composition of the photostationary state (%) of CHP with different irradiation durations and CHP solutions containing 5% Q[8] with different irradiation durations by  $^1\text{H}$  NMR.

catalyst	time	the composition of the photostationary state (%)		
		<i>trans</i> -CHP	<i>cis</i> -CHP	CHP-2
none	0	100	0	0
	30 s	31.16	68.84	0
	10 min	14.68	85.32	0
	60 min	0	51.90	48.10
Q[8]	180min	0	14.39	85.61
	0	100	0	0
	10 s	47.17	52.83	

60 s	29.15	70.85	0
10 min	0	11.11	88.89
20 min	0	0	100

Subsequently, the photochemical behavior of molecular CHP in the presence of Q[8] was characterized by UV-vis absorption spectroscopy. The Q[8]-CHP solution was irradiated at 365nm UV wavelength. As shown in Figure S15, the absorption peak at 345 nm is almost reduced to 0 with the irradiation of ultraviolet light. At this time, only an obvious absorption peak is observed at 222 nm, indicating that CHP is rapidly isomerized from *trans* to *cis* under the action of Q[8], then from *cis* through [2+2] cycloaddition reaction to produce a dimer. This process can be completed within 10 min, much faster than the pure CHP solution of the same concentration. This phenomenon indicates that Q[8] significantly accelerates the photochemical reaction of CHP and enables the photochemical reaction to proceed more completely. In Table 1, the signals of *cis*-CHP and *trans*-CHP are observed in the NMR spectra after the 30s of irradiation; *trans*-CHP accounted for 31.16%, and *cis*-CHP accounted for 68.84%. When the irradiation is continued for 10 minutes, the initial *trans*-CHP is almost converted completely to *cis*-CHP, accounting for 85.32%. When the irradiation is continued for 60 minutes, *cis*-CHP accounted for 51.90%, and CHP-2 accounted for 48.10%. When the irradiation is continued for 180 minutes, the CHP is almost completely converted to a dimer and the *cis*-CHP signal is faintly visible; *cis*-CHP accounted for 14.39%, and CHP-2 accounted for 85.61%. The results showed that Q[8] had a significant promotion effect on the photochemical reactions.

### 2.2.2 Photodimerization of CHP inhibited by Q[7]

To explore the influence of Q[7] on the photoreaction of the guest CHP, the Q[7]-CHP system was irradiated over different durations of UV light in  $\text{D}_2\text{O}$  and the NMR data was recorded. Consistent with the pure CHP solution, the guest CHP changes from *trans*-CHP to *cis*-CHP over 10 min of light irradiation (Figure 5b); *cis*-CHP is still included in the Q[7] cavity. Compared with free *cis*-CHP (Figure 5e), the protons  $\text{H}_d$ ,  $\text{H}_e$ ,  $\text{H}_f$  of the quaternary ammonium and protons  $\text{H}_g$ ,  $\text{H}_h$ ,  $\text{H}_i$ ,  $\text{H}_j$ , and  $\text{H}_k$  of the alkyl chain shift upfield, while the phenol protons  $\text{H}_a$ ,  $\text{H}_b$  and  $\text{H}_c$  shift downfield, indicating that the quaternary ammonium and alkyl chain of *cis*-CHP are included in the cavity of Q[7], while the benzene ring is at the portal of Q[7], with the action mode shown in Figure 5. Interestingly, on continuing to irradiate the system for 60 min (Figure 5c) and 180 min (Figure 5d) no signal of any dimer product is observed after UV irradiation for 180 minutes, indicating that it is included by the Q[7], and is unable to carry out the photo [2+2] cycloaddition reaction. In other words, the cavity of Q[7] inhibits the [2+2] cycloaddition reaction of CHP.

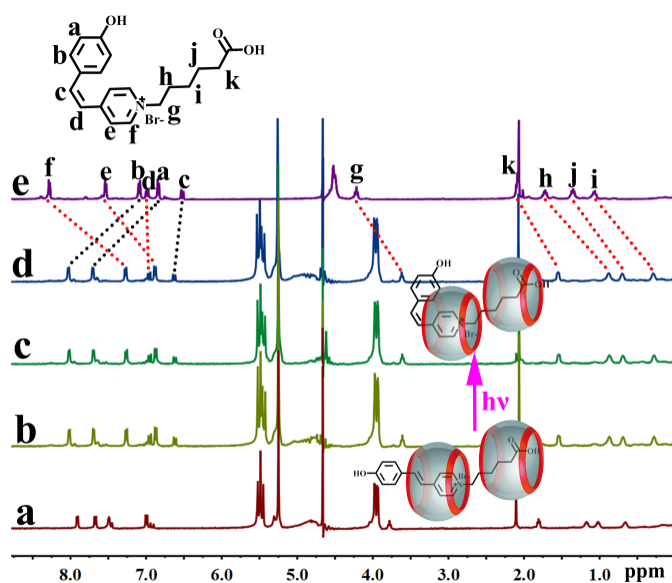


**Figure 5.**  $^1\text{H}$  NMR spectra of Q[7]-CHP solutions ( $5 \times 10^{-4} \text{ mol} \cdot \text{L}^{-1}$ ) in  $\text{D}_2\text{O}$  with different irradiation durations. (a) 0 min; (b) 10 mins; (c) 60 mins; (d) 180 mins. (e) *cis*-CHP.

Since the intrinsic binding ratio of Q[7] and CHP is 2:1, in the Q[7]-CHP solution with a molar ratio of 2:1, almost all CHPs forms host-guest complexes with Q[7] before irradiation. Can the non-stoichiometric ratio of Q[7] inhibit the [2+2] cycloaddition reaction of CHP? Solutions with molar ratios ( $N_{\text{Q}[7]}/N_{\text{CHP}}$ ) of 2:1, 1:1, and 0:1 were subsequently prepared, and the changes of each sample under UV irradiation were monitored to determine the role of Q[7] in this system using UV-vis absorption spectroscopy. As shown in Figure S16, for the 2:1 system in which CHP completely binds with Q[7] before the photoreaction, no absorption peak is observed at 222 nm after UV irradiation, which confirms the inhibition of the photodimerization reaction of CHP molecules by Q[7]. As for the 1:1 and 0:1 systems in which CHP cannot completely bind with Q[7] before the photoreaction, an obvious absorption peak at 222 nm can be observed after UV irradiation. It can be seen that only the CHP included in the cavity of Q[7] cannot carry out the [2+2] cycloaddition reaction, and the part of the CHP that does not form a host-guest complex with Q[7] can still carry out the photodimerization.

### 2.2.3 Analysis of the competitive effect of Q[7] and Q[8]

It can be seen from the above experiments that Q[8] can catalyze the [2+2] cycloaddition reaction of CHP, and Q[7] can inhibit the [2+2] cycloaddition reaction of CHP. To study the photoreaction of CHP when Q[7] and Q[8] coexist, a competitive study was conducted on the system to determine which of Q[7] and Q[8] is more likely to form an inclusion complex. The  $^1\text{H}$  NMR spectrum shown in Figure 6 indicates that Q[8] is added first, the results of which are discussed above. When the molar ratio of Q[8] and CHP is about 0.5 (Figure 6b), then 1.0 equivalent of Q[7] (Figure 6c) and 2.0 equivalent of Q[7] (Figure 6d) are added. When Q[7] is added, compared with the case when the molar ratio of Q[8] to CHP is about 0.5, it is observed that the signals of the protons in the aromatic region shift downfield, while the signals of proton of the alkyl chain shift upfield. This shows that the quaternary ammonium salt and the alkyl chain are included in the cavity of Q[7], while the benzene ring is located at the portal of Q[7] (see cartoon), and Q[8] no longer includes the guest CHP. For comparison, the addition of Q[8] to the solution of Q[7]-CHP inclusion complex is also studied (see Figure S17, supporting information). With the gradual increase of the Q[8] concentration in

the Q[7]-CHP solution, it does not affect the Q[7]-CHP inclusion complex, which is different from the behavior observed when Q[7] is added to the Q[8]-CHP complex. Quantitative data on the host-guest complexation of this system was obtained via isothermal titration calorimetry (ITC) experiments (Figures S7 and S13). The overall binding constant ( $K_a$ ) for the complexation of the CHP guest with the Q[8] host was calculated at  $1.832 \times 10^{12} \text{ M}^{-2}$ , and the CHP guest with the Q[7] host was calculated at  $1.553 \times 10^{13} \text{ M}^{-2}$ , revealing that Q[7] exhibits stronger competition. Both the Q[7]-CHP system and Q[8]-CHP system have relatively large negative enthalpies. A favorable enthalpy change was the main driver toward the formation of the inclusion complex between host Q[8]/Q[7] with guest CHP.

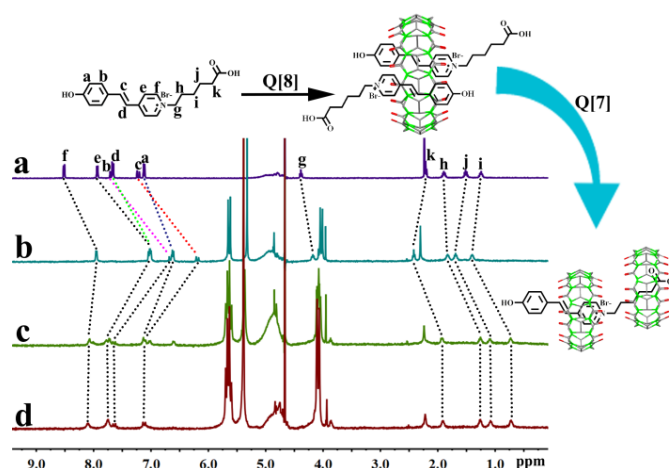


**Figure 6.** Interaction of CHP, Q[7] and Q[8] ( $25^\circ\text{C}$ ): (a)  $^1\text{H}$  NMR spectra (400 MHz,  $\text{D}_2\text{O}$ ) of CHP ( $1.0 \times 10^{-3} \text{ mol} \cdot \text{L}^{-1}$ ); (b) in the presence of Q[8]; (c) adding 1.0 equivalent of Q[7]; (d) and adding 2.0 equivalents of Q[7].

To further study the competition between CHP and Q[7] as well as Q[8], the binding behavior of the host-guest complex was studied by fluorescence emission spectroscopy. As shown in Figure S18, when the host-guest ratio  $n$  ( $N_{\text{Q}[8]}/N_{\text{CHP}}$ ) is fixed at 1:2, and then Q[7] is added to the solution, the fluorescence emission spectrum changes significantly.

### 2.2.4 Photochemical reaction of CHP in the coexistence of Q[7] and Q[8]

The Q[7]-CHP system containing Q[8] solution was irradiated at 365 nm and the NMR spectra were recorded. As shown in Figure 7, the results obtained are consistent with the above experiments (Q[7] inhibits the photodimerization reaction of CHP), and the presence of Q[8] does not affect the photochemical behavior of Q[7]-CHP. Compared with Q[8], the stronger binding force of Q[7] with CHP determines its inhibiting effect on the [2+2] cycloaddition reaction of CHP. Therefore, in the environment of Q[8], Q[7]-CHP will not induce a photo-induced [2+2] cycloaddition reaction.

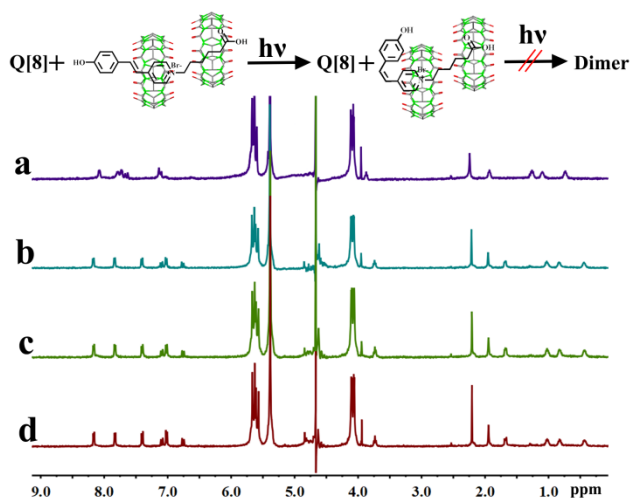


**Figure 7.**  $^1\text{H}$  NMR spectra of Q[7]-CHP solution ( $5 \times 10^{-4} \text{ mol} \cdot \text{L}^{-1}$ ) (containing 50% Q[8]) with different irradiation duration. (a) 0 min; (b) 10 min; (c) 60 min; (d) 180 min.

### 3. Experimental

**Instruments.** Absorption spectra of the host-guest complexes were recorded on an Agilent 8453 spectrophotometer at room temperature. Fluorescence data were recorded on a Varian RF-540 fluorescence spectrophotometer at 293.15 K, whilst NMR spectroscopic data were recorded on a Bruker DPX 400 spectrometer in  $\text{D}_2\text{O}$ . The Isothermal titration calorimetry (ITC) data was obtained using a Nano ITC. The light source of the photoreactor is a MERC-500 mercury lamp light source system.

**Reagents and Chemicals.** The method of synthesizing CHP is shown in the supporting information (Figures S1-S4). The preparation of Q[7] and Q[8] was carried out by using literature methods [42,43]. All chemicals were purchased from Aladdin Reagent Company. Stock solutions of CHP ( $1 \times 10^{-3} \text{ mol/L}$ ) and Q[ $n$ ] ( $n=7, 8$ ) ( $1 \times 10^{-4} \text{ mol/L}$ ) were prepared using doubly-distilled water. The preparation process of the solutions employed herein was to dilute the stock solution to obtain the corresponding concentration standard. This involved initially storing the stock standard solution at room temperature for several weeks before use. The standard working solution is prepared by gradually dripping double distilled water into the standard stock solution. All other chemicals were of analytical reagent grade.

**$^1\text{H}$ NMR measurements.** Experiments were recorded at  $25^\circ\text{C}$ , using a Bruker DPX 400 spectrometer with  $\text{D}_2\text{O}$  as the field frequency lock. The observed chemical shift is reported in parts per million (ppm) relative to the built-in tetramethylsilane (TMS) standard (0.0 ppm).

**Measurement of absorption spectra and fluorescence spectra.** Dilute the stock solution to obtain CHP with a concentration of  $2 \times 10^{-5} \text{ mol} \cdot \text{L}^{-1}$ . These stock solutions were combined to give solutions containing a fixed guest concentration of  $2.0 \times 10^{-5} \text{ mol} \cdot \text{L}^{-1}$  in the presence of different concentrations of Q[ $n$ ] ( $n=7, 8$ ) in each solution. The absorption spectra and fluorescence spectra of each solution were measured. The maximum emission wavelength ( $\lambda_{\text{em}}$ ) of the sample is 457 nm, and the excitation wavelength ( $\lambda_{\text{ex}}$ ) is 350 nm, slit width of 5 nm.

### 4. Conclusions

The host-guest chemical properties between styrylpyridine derivative CHP and Q[7] as well as Q[8] were studied. The results show that the cavity of Q[8] can hold two equivalents of CHP to form Q[8]-CHP(1:2) supramolecular inclusion complexes. For Q[7], CHP is included in the quaternary ammonium and carboxyl parts, respectively, and with two equivalents of Q[7], forms a Q[7]-CHP(2:1) supramolecular inclusion compound. Studies of the photochemical reaction show that the presence of Q[8] can significantly accelerate the photodimerization reaction of CHP, while Q[7] inhibits the photodimerization reaction of CHP, due to the inclusion of Q[7] hindering the bimolecular reaction between CHP molecules. Competitive experiments demonstrate that the formation of the host-guest is more inclined toward Q[7]-CHP. Therefore, when Q[7], Q[8], and CHP coexist, the CHP contained in the cavity of Q[7] cannot bind to Q[8], and thus instead of photodimerization, only the transformation of *cis-trans* isomerism can occur. This research provides us with the potential for designing supramolecular reaction systems to manipulate stereochemistry more rigorously.

### Conflicts of interest

There are no conflicts to declare.

### Acknowledgments

We thank the National Natural Science Foundation of China (NSFC no 21861011), and the Innovation Program for High-level Talents of Guizhou Province (No. 2016-5657) gratefully acknowledged for their financial support. CR thanks the University of Hull for support.

### Notes and references

- [1] H. Murakami, A. Kawabuchi, K. Kotoo, M. Kunitake, and N. Nakashima, A Light-Driven Molecular Shuttle Based on a Rotaxane, *J. Am. Chem. Soc.*, 1997, **119**, 7605-7606.
- [2] G. C. Finnigan, V. Hanson-Smith, T. H. Stevens, J. W. Thornton, Evolution of increased complexity in a molecular machine, *Nature*, 2012, **481**, 360-364.
- [3] M. Schliwa, G. Woehlke, Molecular motors. *Nature*. 2003, **422**, 759-765.
- [4] M. Schliwa, Ed., Molecular Motors, Wiley-VCH, Weinheim, Germany, 2003.
- [5] D. S. Goodsell, Bionanotechnology: Lessons from Nature, Wiley-Liss, Hoboken, NJ, USA 2004.
- [6] R. A. L. Jones, Soft Machines: Nanotechnology and Life, Oxford University Press, Oxford, UK 2008.
- [7] S. J. Chen, Y. C. Wang, T. Nie, C. Y. Bao, C. X. Wang, T. Y. Xu, Q. N. Lin, D. H. Qu, X. Q. Gong, Y. Yang, L. Y. Zhu, and H. Tian, An Artificial Molecular Shuttle Operates in Lipid Bilayers for Ion Transport, *J. Am. Chem. Soc.*, 2018, **140**, 17992-17998.
- [8] A. C. Mendes, E. T. Baran, R. L. Reis, H. S. Azevedo, Self-assembly in nature: using the principles of nature to create complex nanobiomaterials, *Wiley Interdiscip. Rev. Nanomed. Nanobiotechnol.*, 2013, **5**, 582-612.
- [9] D. S. Goodsell, The machinery of life, Copernicus, New York, 2009.

- [10] M. Natali, S. Giordani, Molecular switches as photocontrollable "smart" receptors, *Chem. Soc. Rev.*, 2012, **41**, 4010-4029.
- [11] A. E. Kaifer, Interplay between Molecular Recognition and Redox Chemistry, *Acc. Chem. Res.*, 1999, **32**, 62-71.
- [12] V. P. Torchilin, Multifunctional, stimuli-sensitive nanoparticulate systems for drug delivery, *Nat. Rev. Drug Discovery*, 2014, **13**, 813-827.
- [13] X. Ma, Y. Zhao, Biomedical Applications of Supramolecular Systems Based on Host-Guest Interactions, *Chem. Rev.*, 2015, **115**, 7794-7839.
- [14] V. Blanco, D. A. Leigh, V. Marco, Artificial switchable catalysts, *Chem. Soc. Rev.* 2015, **44**, 5341-5370.
- [15] W. R. Browne, B. L. Feringa, Annu, Light switching of molecules on surfaces, *Rev. Phys. Chem.* 2009, **60**, 407 - 428.
- [16] M. D. Manrique-Juárez, S. Rat, L. Salmon, G. Molnár, C. M. Quintero, L. Nicu, H. J. Shepherd, A. Bousseksou, Switchable molecule-based materials for micro- and nanoscale actuating applications: Achievements and prospects, *Coord. Chem. Rev.*, 2016, **308**, 395-408.
- [17] M. Colaço, P. Máximo, A. J. Parola, N. Basílio, Photoresponsive Binding Dynamics in High-Affinity Cucurbit[8]uril-Dithienylethene Host-Guest Complexes, *Chem. Eur. J.*, 2021, **21**, 9550-9555.
- [18] S. J. Barrow, S. K. Kaser, M. J. Rowland, J. del Barrio, O. A. Scherman, Cucurbituril-Based Molecular Recognition, *Chem. Rev.*, 2015, **115**, 12320-12406.
- [19] K. I. Assaf, W. M. Nau, Cucurbiturils: from synthesis to high-affinity binding and catalysis, *Chem. Soc. Rev.*, 2015, **44**, 394-418.
- [20] M. Liu, J. L. Kan, Y. Q. Yao, Y. Q. Zhang, B. Bian, Z. Tao, Q. J. Zhu, and X. Xiao, Facile preparation and application of luminescent cucurbit[10]uril-based porous supramolecular frameworks, *Sensor Actuat B: Chem.*, 2019, **283**, 290-297.
- [21] R. H. Gao, L. X. Chen, K. Chen, Z. Tao, and X. Xiao, Development of hydroxylated cucurbit[n]urils, their derivatives and potential applications, *Coord. Chem. Rev.*, 2017, **348**, 1-24.
- [22] E. Masson, X. Ling, R. Joseph, L. Kyeremeh-Mensah, X. Lu, Cucurbituril chemistry: a tale of supramolecular success. *RSC Adv.*, 2012, **2**, 1213-1247.
- [23] D. Yang, M. Liu, X. Xiao, Z. Tao, C. Redshaw, Polymeric self-assembled cucurbit[n]urils: Synthesis, structures and applications, *Coord. Chem. Rev.*, 2021, **434**, 213733.
- [24] W. Liu, S. K. Samanta, B. D. Smith, L. Isaacs, Synthetic mimics of biotin/(strept)avidin, *Chem. Soc. Rev.*, 2017, **46**, 2391-2403.
- [25] D. Shetty, J. K. Khedkar, K. M. Park, K. Kim, ChemInform Abstract: Can We Beat the Biotin-Avidin Pair?: Cucurbit[7]uril-Based Ultrahigh Affinity Host-Guest Complexes and Their Applications, *Chem. Soc. Rev.* 2015, **44**, 8747-8761.
- [26] M. Liu, L. X. Chen, P. H. Shan, C. J. Lian, Z. H. Zhang, Y. Q. Zhang, Z. Tao, X. Xiao, Pyridine Detection Using Supramolecular Organic Frameworks Incorporating Cucurbit[10]uril, *ACS Appl. Mater. Inter.*, 2021, **13**, 7434-7442.
- [27] A. E. Kaifer, Toward Reversible Control of Cucurbit[n]uril Complexes, *Acc. Chem. Res.* 2014, **47**, 2160-2167.
- [28] Y. Luo, W. Zhang, M. Liu, J. Zhao, Y. Fan, B. Bian, Z. Tao, Xin Xiao, A supramolecular fluorescent probe based on cucurbit[10]uril for sensing the pesticide dodine, *Chin. Chem. Lett.*, 2021, **32**, 367-370.
- [29] X. Chi, X. Ji, D. Xia, F. Huang, A Dual-Responsive SupraAmphiphilic Polypseudorotaxane Constructed from A Water-Soluble Pillar[7]arene and An Azobenzene-containing Random Copolymer, *J. Am. Chem. Soc.*, 2015, **137**, 1440-1443.
- [30] M. Xue, Y. Yang, X. Chi, X. Yan, F. Huang, Development of Pseudorotaxanes and Rotaxanes: From Synthesis to StimuliResponsive Motions to Applications, *Chem. Rev.* 2015, **115**, 7398-7501.
- [31] D. Xia, P. Wei, B. Shi, F. Huang, A Pillar[6]arene-Based [2]Pseudorotaxane in Solution and in The Solid State and Its PhotoResponsive Self-Assembly Behavior in Solution, *Chem. Commun.*, 2016, **52**, 513-516.
- [32] Y. Hua, A. H. Flood, Flipping the Switch on Chloride Concentrations with a Light-Active Foldamer. *J. Am. Chem. Soc.*, 2010, **132**, 12838-12840.
- [33] K. Zhang, W. Q. Sun, R. L. Lin, X. Xiao, B. Bian, Z. Tao, J. X. Liu, Controlled Encapsulation and Release of an Organic Guest in the Cavity of  $\alpha, \alpha', \delta, \delta'$ -Tetramethylcucurbit[6]uril, *Eur. J. Org. Chem.*, 2019, 1503-1507.
- [34] L. L. Zhu, H. Yan, X-J. Wang, and Y. L. Zhao, Light-Controllable Cucurbit[7]uril-Based Molecular Shuttle, *J. Org. Chem.*, 2012, **77**, 10168-10175.
- [35] B. C. Pemberton, N. Barooah, D. K. Srivatsava, and J. Sivaguru, Supramolecular photocatalysis by confinement-photodimerization of coumarins within cucurbit[8]urils, *Chem. Commun.*, 2010, **46**, 225-227.
- [36] P. Mal, B. Breiner, K. Rissanen, and J. R. Nitschke, White phosphorus is air-stable within a self-assembled tetrahedral capsule. *Science*, 2009, **324**, 1697-1699.
- [37] C. Parente Carvalho, A. Norouzy, V. Ribeiro, W. M. Nau, and U. Pischel, Cucurbiturils as supramolecular inhibitor of DNA restriction by type II endonucleases, *Org. Biomol. Chem.* 2015, **13**, 2866-2869.
- [38] H. Ren, Z. Huang, H. Yang, H. Xu, and X. Zhang, Controlling the reactivity of the Se-Se bond by the supramolecular chemistry of cucurbituril. *Chem. Phys. Chem.* 2015, **16**, 523-527.
- [39] X. C. Hu, F.B. Liu, X. Z. Zhang, Z. Y. Zhao, S. Liu. Expected and unexpected photoreactions of 9-(10-substituted anthracene derivatives in cucurbit[n]uril hosts. *Chem. Sci.*, 2020, **11**, 4779-4785.
- [40] H. Tang, S. S. Thomas, L. Wolf, P. Natarajan, Y. H. Ko, J. Wilson, K. Kim, C. Bohne. Nonlinear Dependence on Na<sup>+</sup> Ions for the Binding Dynamics of Cucurbit[6]uril with the *trans*-1-Methyl-4-(4-hydroxystyryl)pyridinium Cation. *J. Phys. Chem. B*, 2020, **124**, 10219-10225.
- [41] U. Steiner, M. H. Abdel-Kader, P. Fischer, H. E. A. Kramer, Photochemical cis/trans isomerization of a stilbazolium betaine. A protolytic/photochemical reaction cycle, *J. Am. Chem. Soc.*, 1978, **100**, 3190-3197.
- [42] J. Kim, I. S. Jung, S. Y. Kim, E. Lee, J. K. Kang, S. Sakamoto, K. Yamaguchi, K. Kim, New Cucurbituril Homologues: Syntheses, Isolation, Characterization, and X-ray Crystal Structures of Cucurbit[n]uril (n = 5, 7, and 8), *J. Am. Chem. Soc.* 2000, **122**, 540-541.
- [43] S. J. Kim, I. S. Jung, S. Y. Kim, E. Lee, J. Kim, S. Sakamoto, K. Yamaguchi, K. Kim, Macrocycles within macrocycles: cyclen, cyclam, and their transition metal complexes encapsulated in cucurbit[8]uril, *Angew Chem. Int. Ed.* 2001, **40**, 2119-2121.